

Fig. 2 Eutectic $\text{Ca}(\text{NO}_3)_2\text{-RbNO}_3$ (61.2 mol % $(\text{RbNO}_3)_2$) unidirectionally solidified with the same pulling rate and temperature gradient as used in the decomposition of the glass shown in Fig. 1. The lamellae are parallel to the pulling direction. The period is $\sim 6 \mu\text{m}$. Magnification $\times 740$.

cold side. Because of the dependence of the growth rate on the temperature, the growth rate in a reverse gradient is always equal to the pulling rate (provided that the latter is not too high). More details of both techniques will be published elsewhere.

The resulting structures were similar to those obtained from eutectic solidification experiments, but the interphase spacing was smaller by about a factor of ten to twenty by comparison with samples obtained from eutectic solidification at the same pulling rate and temperature gradient (Figs. 1 and 2). X-ray analysis of the decomposed samples showed that the resulting

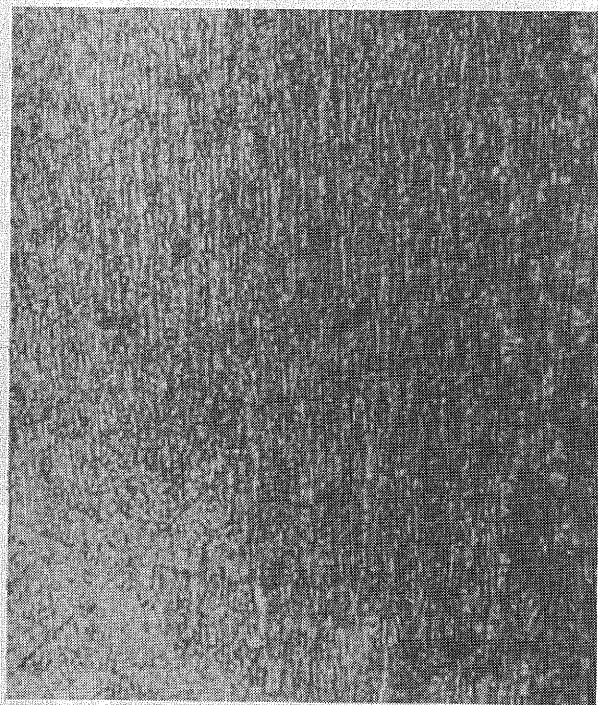


Fig. 3 The system $\text{Bi}_2\text{O}_3\text{-B}_2\text{O}_3$ unidirectionally decomposed from the non-crystalline solid state. The lamellae are parallel to the pulling direction. The period is $\sim 0.4 \mu\text{m}$. Magnification $\times 1,480$.

phases were crystalline and in accordance with the equilibrium phase diagrams.

Another important feature is that quenched-in liquids with compositions far from eutectic (system 2 for example) showed regular lamellar patterns on decomposition, whereas solidification of the melt produced dendritic structures. Also systems without a eutectic or eutectoid point can be used.

It is clear that this extension of the techniques for preparing *in situ* composites offers a great variety of possible composite systems as well as a large range in the volume fractions of the resulting phases.

F. M. A. CARPAY
W. A. CENSE

Philips Research Laboratories,
Eindhoven

Received November 13, 1972.

¹ Livingston, J. D., *Mat. Sci. Eng.*, **7**, 61 (1971).

² Carpay, F. M. A., *Acta Met.*, **18**, 747 (1970).

Controlled Nucleation for the Regulation of the Particle Size in Monodisperse Gold Suspensions

MANY properties of colloids and suspensions depend on the particle size. Series of monodisperse suspensions of the same chemical composition but of rather different particle sizes may be used to study particle size dependent phenomena, such as Brownian motion, light scattering, sedimentation and electrophoresis of small particles. We have used such series to demonstrate the increased tendency of metal suspensions to coagulate in the presence of electrolytes as the radius of the particles increases¹.

From Turkevich's data² we concluded that the reduction of gold chloride with sodium citrate in aqueous solution might be a promising procedure for the preparation of such a set of monodisperse gold suspensions with widely different particle diameters. We hoped by changing the relative amounts of reactants to bring about changes in the relative rates of the two independent processes of nucleation and growth of the metal particles. Whether the available gold is divided over more or fewer nuclei would make a considerable difference for the diameter of the resulting particles. Our expectations were borne out by the experiment.

Fig. 1 shows electron micrographs of six gold suspensions with particle diameters varying from 160 Å to 1500 Å. All six suspensions were prepared by the same simple procedure, the only difference being in the concentration of sodium citrate during the nucleation of the particles.

A standard procedure for obtaining the monodisperse suspension C is as follows. Solutions are prepared of HAuCl_4 (10⁻²% by weight, solution I) and of $\text{Na}_3\text{-citrate}$ (1% by weight, solution II). 50 ml. of solution I is heated to boiling, and 0.50 ml. of solution II is added. In about 25 s the boiling solution turns faintly blue (nucleation). After approximately 70 s the blue colour suddenly changes into a brilliant red,

Table 1 Experimental Data on the Preparation of Mono-disperse Gold Sols

Sol	Amount of Solution II (ml.)	Diameter (Å)	Colour	t_{blue} (s)	t_{red} (s)
A	1.00	160	Orange	25	145
B	0.75	245	Red	25	120
C	0.50	410	Red	25	70
D	0.30	715	dark red*	40	140
E	0.21	975	violet*	60	435
F	0.16	1470	violet*	80	850

* With a yellow Tyndall effect of the scattered light.

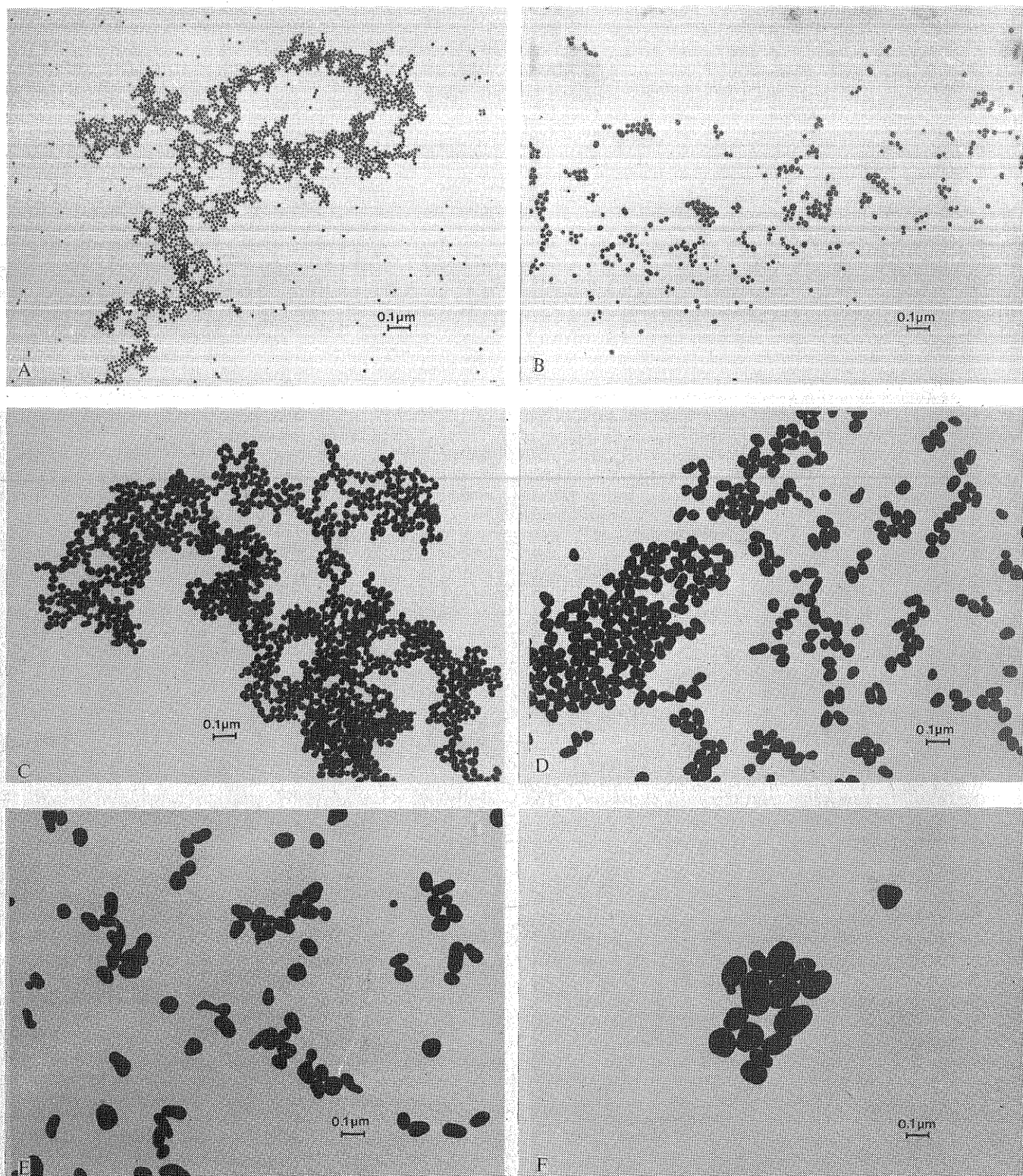


Fig. 1 Electron micrographs of the sols A-F described in Table 1.

indicating the formation of monodisperse spherical particles. Reduction of gold chloride is practically complete after 5 min of boiling. Neither prolonged heating nor the addition of extra citrate produces any substantial change in the suspension after that period.

The monodisperse suspensions with the smaller and with the larger particles are obtained by the same procedure, the only change being in the amount of citrate solution added (Table 1).

The smallest particles obtained in this way had a diameter of 120 Å. The average diameter in the coarsest suspensions

was 1500 Å, obtained with 0.15 ml. of Solution II. At these low citrate levels the results are less reproducible, and boiling has to be continued for at least 30 min to complete the reaction.

The citrate concentration in the standard procedure is such that overall formation of the particles proceeds as rapidly as possible. This concentration is about ten times smaller, and the reaction an order of magnitude faster than under the conditions² which are ordinarily used for the production of colloidal gold. That the resulting particle size in the suspensions is determined by the number of nuclei over which the available gold is divided and is not a result of the reduction of

a different percentage of the available gold with different citrate concentrations was demonstrated in the following way. The average particle size and the size distribution of the suspensions can be determined with great accuracy from electron micrographs. Now assume that in each preparation all the available gold has been reduced—or at least that the gold has been reduced to the same degree in each preparation. This assumption, together with the average volume of a particle which has been determined for each suspension, gives the ratio of the numbers of particles per ml. between any two suspensions. The same ratio can also be obtained independently when the numbers of large and small particles are counted in electron micrographs of a mixture of known aliquots of two suspensions, one with large, the other with small particles. The average radius of the particles in each suspension was determined with an accuracy of about 2% from measurements on 100 or more particles. The ratio of small to large particles in mixed suspensions confirmed the expectations to within 10%. This shows that the assumption of a complete reduction of the gold chloride is reasonable, and that the eventual size of the particles in these mono-disperse suspensions is governed by the number of nuclei which form and grow into particles.

G. FRENS

Philips Research Laboratories,
Eindhoven

Received November 6, 1972.

¹ Frens, G., *Kolloid Z.*, (in the press).

² Turkevich, J., Hillier, J., Stevenson, P. C., *Disc. Farad. Soc.*, **11**, 55 (1951).

Absolute Configuration of a Coupled Chromophore System by Exciton Analysis of Circular Dichroism

THE correct absolute configuration of asymmetric molecules is a problem of fundamental importance in chemistry. The molecular exciton theory of the optical activity on the coupled chromophore system presents an unambiguous method of determining the absolute configuration¹. Triptycene derivatives, which are composed of three substituted benzene chromophores, are optically active when substituted dissymmetrically². The ultraviolet (UV) and the circular dichroism (CD) spectra of chemically correlated (+)-2,5-dimethoxy-7-substituted triptycenes have been systematically investigated and the absolute configuration is deduced as follows.

The characteristics of the CD spectra are illustrated in Fig. 1 on (+)-2,5-dimethoxy-7-dimethylaminotriptycene, where a positive-negative band pair has been observed at the lowest energy region (33,000~37,000 cm⁻¹) and a much stronger one at higher energy region (44,000~47,000 cm⁻¹). It is remarkable that the first ¹B_{2u} type states show a positive CD band irrespective of the nature of substituents, whether electron-donating or accepting. In the ¹B_{2u} absorption region of the dimethoxybenzene and the dimethylaminobenzene rings, the coupled states give a positive and a negative CD band pair. It is important that these transitions are polarized perpendicular to the three-fold symmetry axis of the triptycene skeleton, as predicted by Platt's rule^{3,4} and confirmed by the polarized UV spectral measurement on single crystals^{5,6}.

The optical activity is due to coupling of the transition moments p_i and p_j of the dimethoxybenzene and dimethylaminobenzene rings. In the dimethylaminobenzene ring the centre of the transition moment is displaced towards the substituent group, because the substituent donates π -electrons. This can be verified by the LCAO SCF MO CI calculation on substituted benzenes, in which the centre of the transition dipole is placed on the weighted mean of the transition densities⁷.

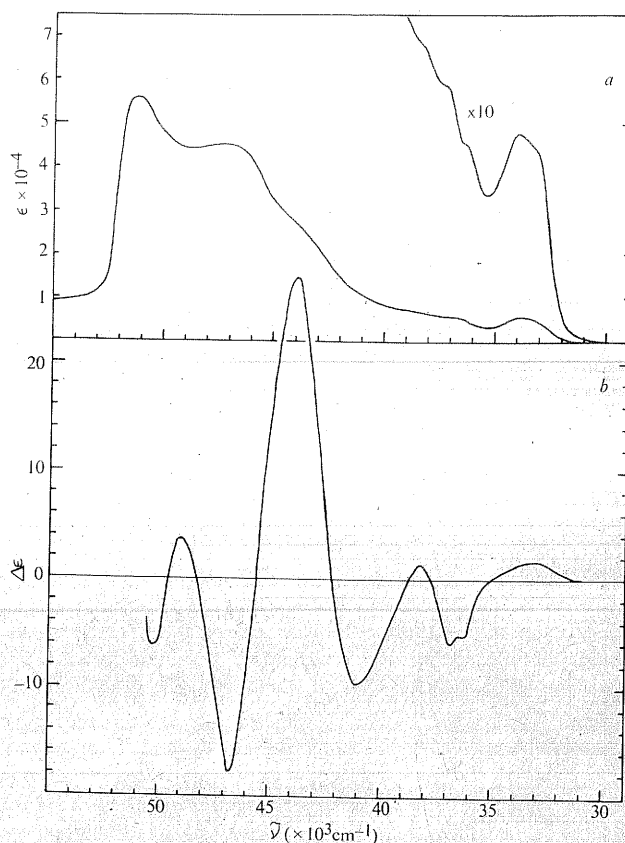


Fig. 1 Ultraviolet (a) and circular dichroism (b) spectra of (+)-2,5-dimethoxy-7-dimethylaminotriptycene.

The rotational strength of the transition from the ground o state to the molecular exciton n state, which is composed of the i -th and the j -th chromophores, is given by^{8,9}

$$R_{on} = \frac{\pi\nu}{c} (R_i - R_j) \cdot p_i \times p_j$$

where R_i and R_j are the positional vectors of the i -th and j -th chromophores and transition moments are defined as follows

$$p_i = \langle o | e r_i | n \rangle \quad \text{and} \quad p_j = \langle n | e r_j | o \rangle$$

For the discussion of the lower energy CD band pair, it is sufficient to consider only the nearly degenerate ¹B_{2u} type states of dimethoxybenzene ring and dimethylaminobenzene ring for all other interactions with higher energy states can be safely neglected. The coupled transitions will be split by the dipole-dipole type exciton interaction, and the transition moments shown in Fig. 2 will give a lower energy band, with a positive rotational strength, and a higher energy band with a negative rotational strength. On this reasoning the absolute configuration with (+)-2,5-dimethoxy-7-dimethylaminotriptycene is deduced as 1S6R as shown in Fig. 1.

The ¹E_{1u} type levels appear in the region higher than 44,000 cm⁻¹ and the degeneracy of the state is removed by the substituent effect. The short-axis polarized ¹E_{1u} type state of the dimethylaminobenzene ring is lower in energy than the long-axis polarized state¹⁰ and the 44,000 cm⁻¹ band is assigned mainly to this origin. This assignment has been confirmed by polarized UV spectral measurements on the single crystal. The centre of the transition dipole is displaced to the substituent with the same direction as that of the ¹B_{2u} state, and the large positive and negative band pair around 45,000 cm⁻¹ can be explained by a similar mechanism. The SCF MO CI calculation on fluorobenzene, however, has shown that the displacement is into the opposite direction because of the strong inductive effect of the fluorine group. Actually